THE JOURNAL OF PHYSICAL CHEMISTRY B

pubs.acs.org/JPCB Article

How Well Does a Solvated Octa-acid Capsule Shield the Embedded Chromophore? A Computational Analysis Based on an Anisotropic Dielectric Continuum Model

Huseyin Aksu, Suranjan K. Paul, John M. Herbert, and Barry D. Dunietz*

Cite This: J. Phys. Chem. B 2020, 124, 6998−7004 Read Online

ACCESS | Metrics & More | Article Recommendations | Supporting Information

ABSTRACT: The optical properties of chromophores embedded in a water-solvated dimer of octa-acid that forms a molecular-shaped capsule are investigated. In particular, we address the anisotropic dielectric environment that appears to blue-shift excitation energies compared to the free aqueous chromophores. Recently we reported that using an effective scalar dielectric constant $\varepsilon \approx 3$ appears to reproduce the measured spectra of the embedded coumarins, suggesting that the capsule provides a significant, albeit not perfect, screening of the aqueous dielectric environment. Here, we report absorption energies using a theoretical treatment that includes continuum solvation affected by an anisotropic dielectric function reflecting the high-dielectric environment outside of the capsule and the low-dielectric region within. We report time-dependent density functional theory calculations using a range-separated functional with the Poisson boundary conditions that model the anisotropic dielectric environment. Our calculations find that the anisotropic environment due to the water-solvated hydrophobic capsule is equivalent to a homogeneous effective dielectric constant of ≈3. The calculated values also appear to reproduce measured absorption of the embedded coumarin, where we study the effect of the hydrophobic capsule on the excited state.

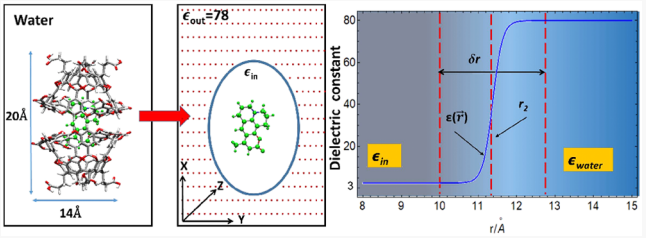

INTRODUCTION

The most widely used implicit solvation models in quantum chemistry are polarizable continuum models (PCMs),[1−5] wherein electrostatic interactions between solute and solvent are included by modeling the latter as a continuous dielectric medium characterized by a scalar dielectric constant, ε. The PCM maps the three-dimensional Poisson equation that describes the continuum electrostatics problem onto a two-dimensional surface charge problem,[4] making it a computationally efficient means to describe a *homogeneous* solvation environment. PCMs have recently been combined with range-separated hybrid (RSH) functionals to describe the heterogeneous solvation environment of the special pair in bacteriochlorophylls,[6,7] in which two semisymmetric branches of pigments are embedded in distinct embedding protein environments, and charge transfer (CT) is understood[8] to proceed down the branch affected by a larger dielectric constant.[9]

For applications such as these, there have been some attempts to implement PCM-like schemes having different dielectric constants (ε_1, ε_2, ...) for distinct spatial regions.[10] PCMs were extended to study solutes at the surface of the solvent.[11−13] A more general version of this idea is to solve a generalized Poisson equation for an environment that is represented by a continuously varying dielectric function, $\varepsilon(\vec{r})$.[14−16] This model, the Poisson equation solver (PEqS), can be used to represent anisotropic solvation environments such as the air/water interface[14,15] and has recently been extended to include the effect of dissolved electrolytes.[16]

In the present work, we use a generalized version of the PEqS to describe electronic excitations of coumarin dyes in an anisotropic solvation environment arising from encapsulation within a supramolecular capsule constituted from a dimer of an octa-acid,[17,18] which is itself solvated in water. Supramolecular systems are often used to encapsulate nonpolar molecules that function as donors in a charge transfer process, with a water-soluble molecule functioning as the acceptor.[18−20] The capsule and the investigated three coumarins are illustrated in Figure 1.

There is wide interest to improve our understanding of the photochemical and photophysical properties, spectroscopy, and CT dynamics of guest organic molecules in confined systems.[21−27] The hydrophobic capsulelike shell formed by the octa-acid dimer shields the embedded chromophores,[21−27] and our own recent computational study finds that an observed blue-shift in the excitation energy upon encapsulation is well

Received: May 5, 2020
Revised: July 15, 2020
Published: August 3, 2020

https://dx.doi.org/10.1021/acs.jpcb.0c04032
J. Phys. Chem. B 2020, 124, 6998−7004

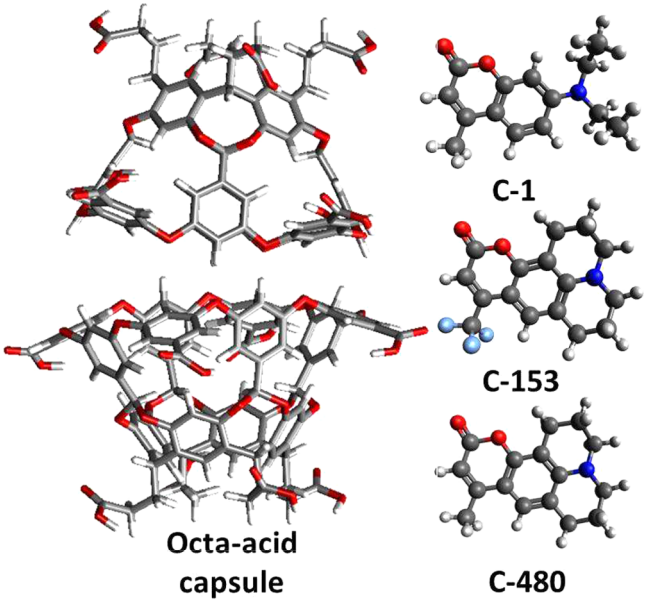

Figure 1. Octa-acid capsule and the guest coumarins: C-1 ($C_{14}H_{17}NO_2$), C-153 ($C_{16}H_{14}F_3NO_2$), and C-480 ($C_{16}H_{17}NO_2$). The atomic coordinates are provided in the Supporting Information.

described by an effective dielectric constant, $\varepsilon_{eff} \approx 3.0$.[28] Operationally, it seems that the capsule environment effectively shields the chromophore from the high-dielectric environment of the aqueous medium, such that the chromophore experiences an effective dielectric constant consistent with expectations for hydrophobic organic matter.

Below we revisit the same system using the PEqS solvation model to examine absorption spectra of guest coumarins C-1, C-153, and C-480 (Figure 1),[18,19] inside the water-solvated octa-acid capsule.[29] The PEqS model affords a more incisive description of the anisotropic solvation environment, in contrast to the PCM approach used in our previous study.[28] To the best of our knowledge this is the first calculation of electronic excited states in an anisotropic dielectric enviornment. We calculate excitation energies for the various coumarins subject to a dielectric constant of ε_{in} inside the capsule (whose value we shall explore) and a dielectric constant $\varepsilon_{out} = 78$ outside, which we fix at the value for water. The dielectric function $\varepsilon(\vec{r})$ used in the PEqS model smoothly interpolates between these two limits, as described in previous work.[15] Figure 2 provides a schematic representation of our computational model. (Contrast with the isotropic picture that involves an effective dielectric constant represented in the inset.)

COMPUTATIONAL PROCEDURE

RSH functionals, also known as long-range corrected (LRC) functionals, have been shown to provide physically meaningful energy levels for frontier molecular orbitals.[30−33] Combinations of such functionals with PCM have been benchmarked successfully to address condensed-phase systems.[30,31,34−36] We employ the LRC-ωPBE functional[37,38] with several PCMs, as described below. The range separation parameter ω is tuned in the gas phase following the J^2 scheme.[39−42] As determined in our previous work,[28] the range separation parameters are 0.020, 0.026, and 0.024 bohr^{-1} for C-1, C-153, and C-480 in $\varepsilon = 78$. For geometries optimized using $\varepsilon = 3$, the corresponding tuned values of ω are 0.072, 0.069, and 0.069 bohr^{-1}.

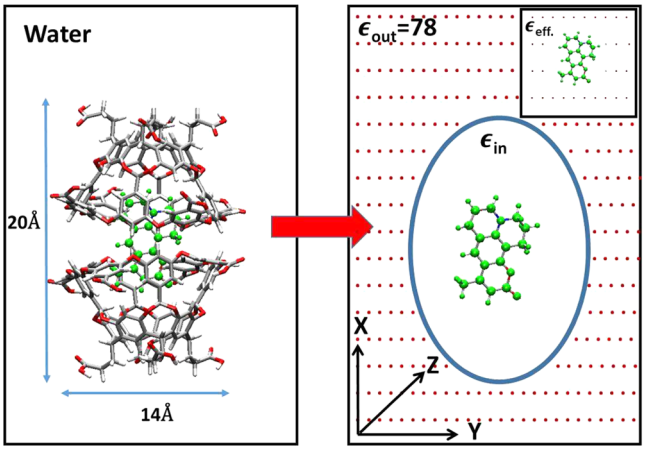

Figure 2. Schematic representation of the dielectric environment for a water-solvated capsule containing a guest coumarin chromophore. Dielectric constants ε_{in} and ε_{out} are associated with spatial regions inside and outside of the capsule volume, respectively, with the latter ($\varepsilon_{out} = 78$) representing aqueous solvation. The insert represents a simpler picture where an effective dielectric constant, ε_{eff}, describes screening due to the water-solvated capsule.[28]

Optimized geometries are also taken from earlier work.[28] All calculations were performed using a locally modified version of the Q-Chem program.[43]

Excited-state energies of the embedded coumarins are computed using time-dependent density functional theory (TDDFT) and the 6-31G(d) basis set unless otherwise noted. The PEqS solvation model[15] is used to polarize the ground-state molecular orbitals and corresponding energy levels, which are subsequently used in the TDDFT framework. In other words, there is no additional excited-state contribution from PEqS, which thus corresponds to a sort of "zeroth-order" solvation approach to TDDFT.[44] For PCMs, one can go beyond this zeroth-order picture by means of a nonequilibrium formalism that incorporates the solvent's response to a sudden change in the electron density of the solute, using the excited-state density and the solvent's optical dielectric constant.[45−48] A perturbation theory, state-specific (ptSS) version of the nonequilibrium PCM formalism has recently been developed by Herbert and co-workers.[44,49,50] The use of perturbation theory avoids certain problems that are normally inherent to state-specific corrections, including convergence difficulties in cases of near degeneracy and lack of orthogonality between the wave functions for different states.[51] One could easily envisage a corresponding PEqS(ptSS) method, but this has not yet been implemented for excitation energies. (A nonequilibrium PEqS approach to vertical ionization has been reported.[14,15]) The integral equation formalism (IEF) version of PCM is used for these calculations,[52,53] as implemented in Q-Chem.[54,55] Solute cavities for IEF-PCM calculations were constructed using the standard procedure of atomic van der Waals (vdW) radii scaled by a factor of 1.2.[4] We will estimate the magnitude of the nonequilibrium correction using TDDFT/PCM(ptSS) calculations for the free aqueous coumarins based on the IEF-PCM. We compared the ptSS approach to an "equilibrium" (or zeroth-order) solvation method in which ground-state molecular orbitals are polarized using the static dielectric constant and then a conventional TD-DFT calculation is performed using these solvent-polarized orbitals, without the nonequilibrium correction that is included at the IEF-

https://dx.doi.org/10.1021/acs.jpcb.0c04032
J. Phys. Chem. B 2020, 124, 6998−7004

PCM(ptSS) level. (This "equilibrium" approach to TD-DFT/PCM has elsewhere been called the "PTE" approach.[50]) For brevity, we refer to the IEF-PCM(ptSS) approach, which includes the nonequilibrium corrections, as simply "ptSS". The optical dielectric constant in the calculations reported below is set to that of water, 1.78.

The PEqS solvation model represents an exact solution (up to discretization errors) to the generalized Poisson equation defined by the dielectric function $\varepsilon(\vec{r})$. As such, this method affords an exact solution to the volume polarization problem in reaction-field theory.[56,57] Volume polarization refers to the fact that the tail of the solute's density penetrates beyond the cavity that separates the atomistic solute from the continuum solute, and the polarization resulting from this tail of the wave function is described only approximately within the IEF-PCM approach.[4,58] On the other hand, IEF-PCM can use a sharp dielectric boundary between solute and solvent, whereas for PEqS this boundary must be smoothed,[14,15] as is also done in classical biomolecular Poisson−Boltzmann electrostatics calculations.[59]

The dielectric function $\varepsilon(\vec{r})$ that is used in the PEqS calculations is constructed by interpolating between limiting values $\varepsilon_{cav} = 1$ (in the atomistic region described by quantum chemistry), ε_{in} (an intermediate value that provides a continuum description of the environment inside of the capsule), and $\varepsilon_{out} = 78$ (representing aqueous solvation outside of the capsule). This interpolation, which is depicted schematically in Figure 3, occurs along vectors $\vec{r}$ that emanate radially from the nuclei. The two separate interpolations are centered at radial distances indicated by r_1 and r_2 in Figure 3. Up to r_1 is the coumarin cavity, which is described at the atomic level using a dielectric constant $\varepsilon = 1$. The boundary at r_1 corresponds to the vdW surface[60] of the coumarin, at which point the continuum environment turns on, with a dielectric constant ε_{in} that is taken to be a parameter of the model, but which has a value representing the hydrophobic capacity of the nonpolar organic capsule. At the surface of the octa-acid capsule (r_2 in Figure 3), the dielectric constant is increased to a value $\varepsilon_{out} = 78$ due to the solvent. We denote this setup as PEqS(ε_{in}:ε_{out}). A two-dimensional contour plot of the dielectric function $\varepsilon(\vec{r})$ around the coumarin chromophore is provided in Figure S1 of the Supporting Information.

The use of two different surfaces to define $\varepsilon(\vec{r})$ is implemented and tested here for the first time, but other details of the PEqS algorithm are the same as the equilibrium solvation approach that is described in ref 15. We use a numerical value $\delta r = 2.75$ Å for the length over which the interpolation of $\varepsilon(\vec{r})$ between limiting values takes place; see Figure 3. A 161 × 161 × 161 Cartesian discretization grid is used for the PEqS calculations, extending between ±20 Å in each dimension for a grid space $\Delta x = 0.25$ Å, consistent with previous convergence tests.[15] Below, the PEqS models are compared to simplified models noted as "PEqS*". The PEqS* models are obtained by replacing the capsule surface with a single sphere of radius set to 10 Å or as noted. Another (1:78) PEqS* model is achieved by significantly increasing the atomic vdW radii by a factor of 10 or as noted. We also set up (1:ε) models by increasing the atomic radii in IEF-PCM and IEF-PCM(ptSS) calculations. We indicate these (1:ε) calculations below as "IEF*" and "ptSS*". In particular, we are using the IEF* and ptSS* (with the significantly larger atomic radii) to compare to PEqS(1:78) and PEqS(1:3). (We emphasize that IEF*/PtSS* and PEqS* establish simplified (1:78) setups for representing a coumarin captured within a perfectly screened region by increasing the molecular solute surface. Indeed, the PEqS* results as shown below are in excellent agreement with the PEqS (1:78) values that are based on the actual capsule surface for generating the dielectric interface. The PEqS* values do not appear to depend significantly on the actual factor increasing the atomic radii or the sphere size used in setting up these models.)

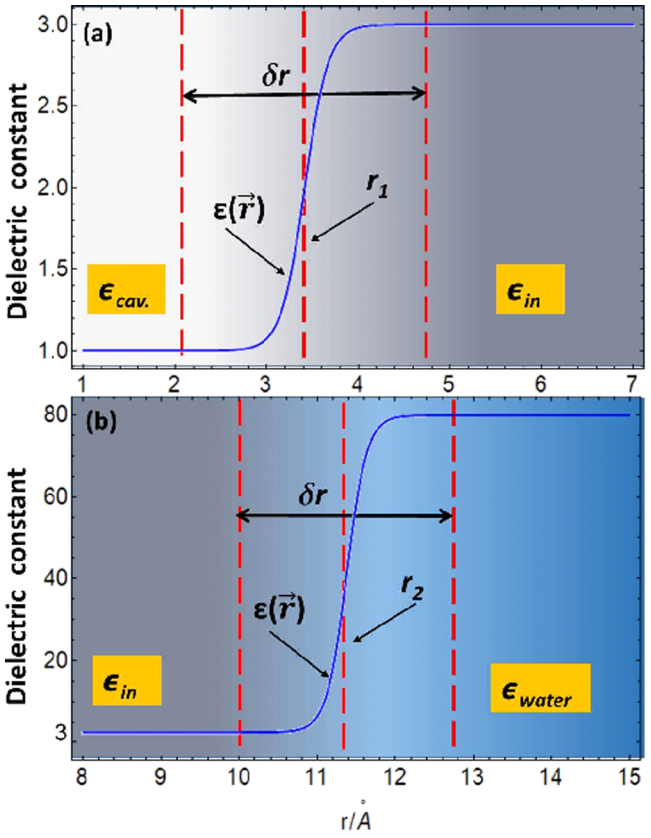

Figure 3. Illustration of the interpolation (between limiting values $\varepsilon_{cav} = 1$, ε_{in}, and $\varepsilon_{out} = 78$) that is used to define the dielectric function $\varepsilon(\vec{r})$ for PEqS(1:78) calculations. This interpolation takes place along vectors pointing radially outward from the center of a coumarin atom, according to the following procedure. (a) A first interpolation between $\varepsilon = 1$ and $\varepsilon = \varepsilon_{in}$ (represented here by the value $\varepsilon_{in} = 3$) is centered at the boundary of the vdW surface,[60] i.e., r_1 represents an atomic vdW radius. (b) A second interpolation to a value $\varepsilon = 78$ occurs at a distance r_2 that represents the boundary of the molecular capsule. In both cases, the length of the interpolation is taken to be $\delta r = 2.75$ Å.

RESULTS AND DISCUSSIONS

PCMs describe the solute−solvent electrostatic interactions in terms of a single, scalar dielectric constant (ε) for a continuum environment that is assumed to be isotropic. In previous work,[28] we described the effects of electrostatic screening by the octa-acid capsule using an effective dielectric constant (ε_{eff}) that was obtained by systematically varying ε from its gas-phase value ($\varepsilon = 1$) to its aqueous value ($\varepsilon = 78$), comparing the TDDFT/PCM excitation energies to values measured experimentally for coumarins enclosed in the octa-acid capsule. Experimentally measured shifts in the excitation energies, relative to free coumarins in aqueous solution, are reproduced quite well by an effective dielectric constant $\varepsilon_{eff} = 3$.[28] (We

https://dx.doi.org/10.1021/acs.jpcb.0c04032
J. Phys. Chem. B 2020, 124, 6998−7004

compare calculated vertical excitations to maxima of the measured spectral bands.[19])

Before we proceed to consider a more meaningful anisotropic dielectric function, we first consider the free coumarins in aqueous solution using several different solvation models. These are listed in Table 1 for both ε = 78 and the previously determined effective value of ε = 3. (cc-pVTZ values listed in Supporting Information Table S1 are within 0.05−0.1 eV lower, and 6-31+G(d) values are at around 0.1 eV lower). We note that the equilibrium versions of IEF-PCM energies are in good agreement with those obtained using PEqS solvation, with differences smaller than 0.03 eV. This comparison indicates that differences related to the treatment of volume polarization, discretization, and the smoothing of the dielectric function at the solute/continuum interface have very small numerical effects. In addition, we note that the nonequilibrium (ptSS) correction to the equilibrium IEF-PCM solvation energy ranges from −0.02 to −0.04 eV.

Table 1. TDDFT Excitation Energies (eV) of Free Solvated Coumarins Using Various Isotropic Continuum Solvation Models[a]

			TDDFT		
			IEF-PCM		
ε	coumarin	expt.	ptSS	equilibrium	PEqS
3	C-1		3.41	3.45	3.48
	C-153		3.06	3.09	3.11
	C-480		3.23	3.26	3.27
78	C-1	3.26[b]	3.22	3.26	3.28
	C-153	2.88[b]	2.91	2.93	2.94
	C-480	3.13[b]	3.11	3.13	3.13

[a]See Supporting Information Table S1 for cc-pVTZ and 6-31+G(d) based energies. Measured values in solvated capsule are discussed in the main text. [b]For the free coumarin in water.[61]

Next we address the absorption energies of the guest coumarins, using the function $\varepsilon(\vec{r})$ in the anisotropic PEqS (ε_{in}:ε_{out}) calculations as described above; see energies listed in Table 2. We first note that TDDFT/PEqS(1:78) excitation energies are equivalent within 0.05 eV to the simpler PEqS* setup based on increasing vdW atomic radii and additional (1:3) energies included in Supporting Information Table S2, indicating that there is only a weak dependence of the calculated excitation energies on the actual setup of $\varepsilon(\vec{r})$ for addressing the dielectric interface due to the molecular capsule. Also important is the observation that the PEqS*(1:78) energies agree with the corresponding IEF* energies to within 0.001 eV, which presents a significantly tighter agreement than in the isotropic cases described above. (The IEF* values were obtained by increasing the vdW atomic radii by a scale factor of 10.) In addition, we find that the IEF-ptSS* energies bear a negligible nonequilibrium correction that is in all cases smaller in absolute value than 0.001 eV compared to the already small ptSS correction of about 0.02 eV in the isotropic cases. Additional PEqS(1:3) values, demonstrating a similar trend, are listed in Supporting Information Table S2. Also included in Table S2 are (1:78) energies obtained using 6-31+G(d) that are consistently around 0.1 eV smaller than the 6-31G(d) energies, similar to the basis set trend found above for the free solvated coumarins in Table 1.

Table 2. TDDFT Excitation Energies (in eV) Using the Anisotropic (1:78) Solvation Model[a]

coumarin	PEqS	PEqS*[b]/IEF*[b]
C-1	3.43	3.47
C-153	3.08	3.13
C-480	3.26	3.27

[a]Additional values obtained at the 6-31+G(d) basis set and anisotropic (1:3) model are provided in Supporting Information Table S2. Nonequilibrium correction calculated using the ptSS* level is smaller than 0.001 eV in absolute value in all cases. [b]Using increased atomic radii.

We also address the effect of the coumarin to move within the capsule cavity, by rotating the molecules about the main axis of the capsule that is of an ellipsoid shape (see illustration in Supporting Information Figure S2). As shown in Supporting Information Table S3, the excitation energies remain within 0.05 eV for the three considered orientations. We note that fully quantifying the flexibility of the coumarins to move within the capsule remains an open question. Similarly the effect of cocapturing solvent molecules within the cavity is another important aspect that should be addressed in future studies.

TDDFT/PEqS(1:78) excitation energies are in good agreement with those obtained using a single, isotropic dielectric constant of ε_{eff} = 3, with differences of less than 0.05 eV as seen in Table 3. (Here, PEqS* values, which are within 0.02 eV from the PEqS values, were obtained using a sphere to form the outer interface starting at 10 Å. Results with spheres of other radii are included in Supporting Information Table S4.) We therefore find that an anisotropic dielectric environment, where the coumarin is embedded within a perfectly hydrophobic molecular capsule in aqueous solution, corresponds closely to a homogeneous environment of $\varepsilon_{eff} \approx 3$. This is in agreement with the finding of our previous study.[28] Furthermore, we find that TDDFT/PEqS(1:78) excitation energies are in good agreement with the measured values for C-1 and C-480, suggesting that the hydrophobic capsule perfectly shields water's solvation effects from the coumarin, which therefore experiences a dielectric environment more consistent with nonpolar organic matter. However, in the case of C-153, the TDDFT/PEqS(1:78) result overestimates experiment by 0.2 eV. As reported before, the excitation energies tend to red-shift as the dielectric constant is increased.[28] Indeed we find that an increase of ε_{in} lowers the C-153 excitation from 3.08 to 2.99 eV with ε_{in} = 2 and further reduces it to 2.96 eV with ε_{in} = 3.

Table 3. TDDFT Excitation Energies for Encapsulated Coumarins

		TDDFT			
coumarin	expt.[a]	PEqS (ε_{eff} = 3)[c]	PEqS*[b] (1:78)	PEqS (1:78)[d]	PEqS*[b] (3:78)
C-1	3.43	3.48	3.46	**3.43**	3.30
C-153	2.93	3.11	3.13	3.08	**2.96**
C-480	3.28	3.27	3.27	**3.26**	3.14

[a]From refs 19 and 28. [b]Using a spherical outer interface. Other choices for the radius can be found in Supporting Information Table S4. [c]Using a single vdW cavity for the coumarin. [d]Using (ε_{in}:ε_{out}) as described in the text.

The different behavior indicated for C-153, where the capsule is not perfectly hydrophobic, may result from the

https://dx.doi.org/10.1021/acs.jpcb.0c04032
J. Phys. Chem. B 2020, 124, 6998−7004

electronegative fluorine atoms, which the molecular capsule can only partially shield. The collective Mulliken charge of the three fluorine atoms in C-153 is −0.69*e* while that of the carbon atom in the CF_3 moiety is +0.71*e*. In comparison, Mulliken charge on carbon in the corresponding CH_3 group of C-1 and C-480 is about −0.6*e*. The resulting molecular dipoles are presented in Supporting Information Figure S3. The effect of fluorination in C-153 is to align the dipole along the main molecular axis, whereas for C-1 and C-480 the dipole moment is skewed in relation to the axis of the benzopyrone moiety.

CONCLUSIONS

Excitation energies of coumarins embedded within a molecular capsule formed from an octa-acid dimer are computed using TDDFT with various continuum solvation models, including one based on an anisotropic dielectric function, $\varepsilon(\vec{r})$.[15] The molecular capsule forms a hydrophobic shell, within which nonpolar organic chromophores can be inserted, forming one-half of a solvated donor−acceptor pair for photoinduced CT reactions in aqueous solution.[17−19,62] The PeqS allows to directly study the role of the hydrophobic capsule to screen the solvent dielectric and affect the electronic excitation energies of the captured chromophores. Using the generalized PEqS,[15] we can model the environment around the encapsulated chromophore in terms of an inner, low-dielectric environment along with an outer, high-dielectric environment representing aqueous solvation.

In practice, we find that the anisotropic description is equivalent to an earlier model[28] in which the coumarin dye is surrounded by a homogeneous dielectric environment characterized by a single, effective dielectric constant $\varepsilon_{\text{eff}} = 3$. Computed excitation energies are in good agreement with those measured experimentally for the aqueous host−guest system. In the case of C-153, the electronegative CF_3 moiety appears to diminish the hydrophobic capacity of the capsule.

ASSOCIATED CONTENT

Supporting Information

The Supporting Information is available free of charge at https://pubs.acs.org/doi/10.1021/acs.jpcb.0c04032.

Tables of larger basis set energies, PEqS* and IEF* energies, and upon rotation; figures of $\varepsilon(\vec{r})$ with the sphere setup, coumarin dipole orientations, and rotated coumarins (PDF)

AUTHOR INFORMATION

Corresponding Author

Barry D. Dunietz − *Department of Chemistry and Biochemistry, Kent State University, Kent, Ohio 44242, United States;* orcid.org/0000-0002-6982-8995; Phone: +1 330 6722032; Email: bdunietz@kent.edu; Fax: +1 330 6723816

Authors

Huseyin Aksu − *Department of Physics, Canakkale Onsekiz Mart University, 17100 Canakkale, Turkey; Department of Chemistry and Biochemistry, Kent State University, Kent, Ohio 44242, United States;* orcid.org/0000-0001-9463-3236

Suranjan K. Paul − *Department of Chemistry and Biochemistry, The Ohio State University, Columbus, Ohio 43210, United States*

John M. Herbert − *Department of Chemistry and Biochemistry, The Ohio State University, Columbus, Ohio 43210, United States;* orcid.org/0000-0002-1663-2278

Complete contact information is available at: https://pubs.acs.org/10.1021/acs.jpcb.0c04032

Notes

The authors declare no competing financial interest.

ACKNOWLEDGMENTS

Computing facilities were provided by the Ohio Supercomputer Center[63] (projects PAA-0003 and PAA-0213 awarded to J.M.H. and B.D.D., respectively) and by the Kent State University College of Arts and Sciences. Work by S.K.P. and J.M.H. was supported by National Science Foundation grant no. CHE-1665322. Work by H.A. and B.D.D. was supported by the Department of Energy, basic energy sciences grant no. DE-SC0016501.

REFERENCES

(1) Tomasi, J.; Mennucci, B.; Cammi, R. Quantum Mechanical Continuum Solvation Models. *Chem. Rev.* **2005**, *105*, 2999−3094.

(2) Cramer, C. J.; Truhlar, D. G. A Universal Approach to Solvation Modeling. *Acc. Chem. Res.* **2008**, *41*, 760−768.

(3) Mennucci, B. Polarizable Continuum Model. *WIREs Comput. Mol. Sci.* **2012**, *2*, 386−404.

(4) Herbert, J. M.; Lange, A. W. In *Many-Body Effects and Electrostatics in Biomolecules*; Cui, Q., Ren, P., Meuwly, M., Eds.; Pan Stanford Publishing: Singapore, 2016; Chapter 11, pp 363−416.

(5) Klamt, A. The COSMO and COSMO-RS Solvation Models. *Wiley Interdiscip. Rev.: Comput. Mol. Sci.* **2018**, *8*, No. e1338.

(6) Aksu, H.; Schubert, A.; Geva, E.; Dunietz, B. D. Explaining Spectral Asymmetries and Excitonic Characters of the Core Pigment Pairs in the Bacterial Reaction Center Using Screened Range-Separated Hybrid Functionals. *J. Phys. Chem. B* **2019**, *123*, 8970−8975.

(7) Aksu, H.; Schubert, A.; Bhandari, S.; Yamada, A.; Geva, E.; Dunietz, B. D. On the Role of the Special Pair in Photosystems as a Charge Transfer Rectifier. *J. Phys. Chem. B* **2020**, *124*, 1987−1994.

(8) Niedringhaus, A.; Policht, V. R.; Sechrist, R.; Konar, A.; Laible, P. D.; Bocian, D. F.; Holten, D.; Kirmaier, C.; Ogilvie, J. P. Primary Processes in the Bacterial Reaction Center Probed by Two-Dimensional Electronic Spectroscopy. *Proc. Natl. Acad. Sci. U. S. A.* **2018**, *115*, 3563−3568.

(9) Steffen, M. A.; Lao, K.; Boxer, S. G. Dielectric Asymmetry in the Photosynthetic Reaction Center. *Science* **1994**, *264*, 810−816.

(10) Hoshi, H.; Sakurai, M.; Inoue, Y.; Chûjô, R. Medium Effects on the Molecular Electronic Structure: Part 2. The Application of the Theory of Medium Effects in the Framework of the CNDO and INDO Methods. *J. Mol. Struct.: THEOCHEM* **1988**, *180*, 267−281.

(11) Frediani, L.; Cammi, R.; Corni, S.; Tomasi, J. A Polarizable Continuum Model for Molecules at Diffuse Interfaces. *J. Chem. Phys.* **2004**, *120*, 3893−3907.

(12) Mozgawa, K.; Mennucci, B.; Frediani, L. Solvation at Surfaces and Interfaces: A Quantum-Mechanical/Continuum Approach Including Nonelectrostatic Contributions. *J. Phys. Chem. C* **2014**, *118*, 4715−4725.

(13) Bondesson, L.; Frediani, L.; Agren, H.; Mennucci, B. Solvation of N3- at the Water Surface: The Polarizable Continuum Model Approach. *J. Phys. Chem. B* **2006**, *110*, 11361−11368.

(14) Coons, M. P.; You, Z.-Q.; Herbert, J. M. The Hydrated Electron at the Surface of Neat Liquid Water Appears to be Indistinguishable from the Bulk Species. *J. Am. Chem. Soc.* **2016**, *138*, 10879−10886.

(15) Coons, M. P.; Herbert, J. M. Quantum Chemistry in Arbitrary Dielectric Environments: Theory and Implementation of Non-

equilibrium Poisson Boundary Conditions and Application to Compute Vertical Ionization Energies at the Air/Water Interface. *J. Chem. Phys.* **2018**, *148*, 222834.
(16) Stein, C. J.; Herbert, J. M.; Head-Gordon, M. The Poisson-Boltzmann Model for Implicit Solvation of Electrolyte Solutions: Quantum Chemical Implementation and Assessment via Sechenov Coefficients. *J. Chem. Phys.* **2019**, *151*, 224111.
(17) Porel, M.; Chuang, C.-H.; Burda, C.; Ramamurthy, V. Ultrafast Photoinduced Electron Transfer Between an Incarcerated Donor and a Free Acceptor in Aqueous Solution. *J. Am. Chem. Soc.* **2012**, *134*, 14718−14721.
(18) Chuang, C.-H.; Porel, M.; Choudhury, R.; Burda, C.; Ramamurthy, V. Ultrafast Electron Transfer Across a Nanocapsular Wall: Coumarins as Donors, Viologen as Acceptor, and Octa Acid Capsule as the Mediator. *J. Phys. Chem. B* **2018**, *122*, 328−337.
(19) Gupta, S.; Adhikari, A.; Mandal, A. K.; Bhattacharyya, K.; Ramamurthy, V. Ultrafast Singlet−Singlet Energy Transfer between an Acceptor Electrostatically Attached to the Walls of an Organic Capsule and the Enclosed Donor. *J. Phys. Chem. C* **2011**, *115*, 9593−9600.
(20) Li, Y. Molecular Design of Photovoltaic Materials for Polymer Solar Cells: Toward Suitable Electronic Energy Levels and Broad Absorption. *Acc. Chem. Res.* **2012**, *45*, 723−733.
(21) Ramamurthy, V. *Photochemistry in Organized: Constrained Media*; VCH: New York, 1991.
(22) Yoshizawa, M.; Fujita, M. Self-Assembled Coordination Cage as a Molecular Flask. *Pure Appl. Chem.* **2005**, *77*, 1107−1112.
(23) Turro, N. J. Fun with Photons, Reactive Intermediates, and Friends. Skating on the Edge of the Paradigms of Physical Organic Chemistry, Organic Supramolecular Photochemistry, and Spin Chemistry. *J. Org. Chem.* **2011**, *76*, 9863.
(24) Ramamurthy, V.; Gupta, S. Supramolecular Photochemistry: from Molecular Crystals to Water-Soluble Capsules. *Chem. Soc. Rev.* **2015**, *44*, 119−135.
(25) Ramamurthy, V.; Inoue, Y. *Supramolecular Photochemistry*; John Wiley: Hoboken, NJ, 2011.
(26) Brinker, U. H.; Mieusset, J.-L. *Molecular Encapsulation*; John Wiley and Sons: Chichester, U.K., 2010.
(27) Das, A.; Sharma, G.; Kamatham, N.; Prabhakar, R.; Sen, P.; Ramamurthy, V. Ultrafast Solvation Dynamics Reveal that Octa Acid Capsule's Interior Dryness Depends on the Guest. *J. Phys. Chem. A* **2019**, *123*, 5928−5936.
(28) Bhandari, S.; Zheng, Z.; Maiti, B.; Chuang, C.-H.; Porel, M.; You, Z.-Q.; Ramamurthy, V.; Burda, C.; Herbert, J. M.; Dunietz, B. D. What Is the Optoelectronic Effect of the Capsule on the Guest Molecule in Aqueous Host/Guest Complexes? A Combined Computational and Spectroscopic Perspective. *J. Phys. Chem. C* **2017**, *121*, 15481−15488.
(29) Porel, M.; Jayaraj, N.; Kaanumalle, L. S.; Maddipatla, M. V. S. N.; Parthasarathy, A.; Ramamurthy, V. Cavitand Octa Acid Forms a Nonpolar Capsuleplex Dependent on the Molecular Size and Hydrophobicity of the Guest. *Langmuir* **2009**, *25*, 3473−3481.
(30) Phillips, H.; Zheng, Z.; Geva, E.; Dunietz, B. D. Orbital Gap Predictions for Rational Design of Organic Photovoltaic Materials. *Org. Electron.* **2014**, *15*, 1509−1520.
(31) Phillips, H.; Geva, E.; Dunietz, B. D. Calculating Off-Site Excitations in Symmetric Donor-Acceptor Systems Via Time-Dependent Density Functional Theory With Range-Separated Density Functionals. *J. Chem. Theory Comput.* **2012**, *8*, 2661−2668.
(32) Stein, T.; Autschbach, J.; Govind, N.; Kronik, L.; Baer, R. Curvature and Frontier Orbital Energies in Density Functional Theory. *J. Phys. Chem. Lett.* **2012**, *3*, 3740−3744.
(33) Kronik, L.; Stein, T.; Refaely-Abramson, S.; Baer, R. Excitation Gaps of Finite-Sized Systems from Optimally Tuned Range-Separated Hybrid Functionals. *J. Chem. Theory Comput.* **2012**, *8*, 1515−1531.
(34) Bhandari, S.; Cheung, M.; Geva, E.; Kronik, L.; Dunietz, B. D. Fundamental Gaps of Condensed-Phase Organic Semiconductors From Single-Molecule Polarization-Consistent Optimally Tuned Screened Range-Separated Hybrid Functionals. *J. Chem. Theory Comput.* **2018**, *14*, 6287−6294.
(35) Bhandari, S.; Dunietz, B. D. Quantitative Accuracy in Calculating Charge Transfer State Energies in Solvated Molecular Dimers Using Screened Range Separated Hybrid Functional Within a Polarized Continuum Model. *J. Chem. Theory Comput.* **2019**, *15*, 4305.
(36) Begam, K.; Bhandari, S.; Maiti, B.; Dunietz, B. D. Screened Range-Separated Hybrid Functional with Polarizable Continuum Model Overcomes Challenges in Describing Triplet Excitations in the Condensed Phase Using TDDFT. *J. Chem. Theory Comput.* **2020**, *16*, 3287.
(37) Vydrov, O. A.; Scuseria, G. E. Assessment of a Long-Range Corrected Hybrid Functional. *J. Chem. Phys.* **2006**, *125*, 234109−234117.
(38) Rohrdanz, M. A.; Martins, K. M.; Herbert, J. M. A Long-Range-Corrected Density Functional That Performs Well for Both Ground-State Properties and Time-Dependent Density Functional Theory Excitation Energies, Including Charge-Transfer Excited States. *J. Chem. Phys.* **2009**, *130*, 054112−054119.
(39) Refaely-Abramson, S.; Sharifzadeh, S.; Jain, M.; Baer, R.; Neaton, J. B.; Kronik, L. Gap Renormalization of Molecular Crystals From Density-Functional Theory. *Phys. Rev. B: Condens. Matter Mater. Phys.* **2013**, *88*, No. 081204(R).
(40) Kuritz, N.; Stein, T.; Baer, R.; Kronik, L. Charge-Transfer-Like $\pi \rightarrow \pi^*$ Excitations in Time-Dependent Density Functional Theory: A Conundrum and Its Solution. *J. Chem. Theory Comput.* **2011**, *7*, 2408−2415.
(41) Stein, T.; Kronik, L.; Baer, R. Prediction of Charge-Transfer Excitations in Coumarin-Based Dyes Using a Range-Separated Functional Tuned From First Principles. *J. Chem. Phys.* **2009**, *131*, 244119.
(42) Grimme, S.; Neese, F. Double-hybrid density functional theory for excited electronic states of molecules. *J. Chem. Phys.* **2007**, *127*, 154116.
(43) Shao, Y.; Gan, Z.; Epifanovsky, E.; Gilbert, A. T. B.; Wormit, M.; Kussmann, J.; Lange, A. W.; Behn, A.; Deng, J.; Feng, X.; et al. Advances in Molecular Quantum Chemistry Contained in the Q-Chem 4 Program Package. *Mol. Phys.* **2015**, *113*, 184−215.
(44) You, Z.-Q.; Mewes, J.-M.; Dreuw, A.; Herbert, J. M. Comparison of the Marcus and Pekar Partitions in the Context of Non-Equilibrium, Polarizable-Continuum Solvation Models. *J. Chem. Phys.* **2015**, *143*, 204104.
(45) Cammi, R.; Tomasi, J. Nonequilibrium Solvation Theory for the Polarizable Continuum Model: A New Formulation at the SCF Level with Application to the Case of the Frequency-Dependent Linear Electric Response Function. *Int. J. Quantum Chem.* **1995**, *56*, 465−474.
(46) Cossi, M.; Barone, V. Separation Between Fast and Slow Polarizations in Continuum Solvation Models. *J. Phys. Chem. A* **2000**, *104*, 10614−10622.
(47) Improta, R.; Barone, V.; Scalmani, G.; Frisch, M. J. A State-Specific Polarizable Continuum Model Time Dependent Density Functional Theory Method for Excited State Calculations in Solution. *J. Chem. Phys.* **2006**, *125*, 054103.
(48) Cammi, R. Coupled-Cluster Theories for the Polarizable Continuum Model. II. Analytical Gradients for Excited States of Molecular Solutes by the Equation of Motion Coupled-Cluster Method. *Int. J. Quantum Chem.* **2010**, *110*, 3040−3052.
(49) Mewes, J.-M.; You, Z.-Q.; Wormit, M.; Kriesche, T.; Herbert, J. M.; Dreuw, A. Experimental Benchmark Data and Systematic Evaluation of Two a Posteriori, Polarizable-Continuum Corrections for Vertical Excitation Energies in Solution. *J. Phys. Chem. A* **2015**, *119*, 5446−5464.
(50) Mewes, J.-M.; Herbert, J. M.; Dreuw, A. On the Accuracy of the State-Specific Polarizable Continuum Model for the Description of Correlated Ground and Excited States in Solution. *Phys. Chem. Chem. Phys.* **2017**, *19*, 1644−1654.

https://dx.doi.org/10.1021/acs.jpcb.0c04032
J. Phys. Chem. B 2020, 124, 6998−7004

(51) Jacobson, L. D.; Herbert, J. M. A Simple Algorithm for Determining Orthogonal, Self-Consistent Excited-State Wave Functions for a State-Specific Hamiltonian: Application to the Optical Spectrum of the Aqueous Electron. *J. Chem. Theory Comput.* **2011**, *7*, 2085−2093.
(52) Mennucci, B.; Tomasi, J. Continuum Solvation Models: A new Approach to the Problem of Solute's Charge Distribution and Cavity Boundaries. *J. Chem. Phys.* **1997**, *106*, 5151−5158.
(53) Mennucci, B.; Cancés, E.; Tomasi, J. Evaluation of Solvent Effects in Isotropic and Anisotropic Dielectrics and in Ionic Solutions with a Unified Integral Equation Method, Theoretical Bases, Computational Implementation, and Numerical Applications. *J. Phys. Chem. B* **1997**, *101*, 10506−10517.
(54) Lange, A. W.; Herbert, J. M. A Smooth, Nonsingular, and Faithful Discretization scheme for Polarizable Continuum Models: The Switching/Gaussian Approach. *J. Chem. Phys.* **2010**, *133*, 244111.
(55) Lange, A. W.; Herbert, J. M. Symmetric versus Asymmetric Discretization of the Integral Equations in Polarizable Continuum Solvation Models. *Chem. Phys. Lett.* **2011**, *509*, 77−78.
(56) Chipman, D. M. Charge Penetration in Dielectric Models of Solvation. *J. Chem. Phys.* **1997**, *106*, 10194−10206.
(57) Zhan, C.-G.; Bentley, J.; Chipman, D. M. Volume Polarization in Reaction Field Theory. *J. Chem. Phys.* **1998**, *108*, 177−192.
(58) Chipman, D. M. Reaction Field Treatment of Charge Penetration. *J. Chem. Phys.* **2000**, *112*, 5558−5565.
(59) Grant, J. A.; Pickup, B. T.; Nicholls, A. A Smooth Permittivity Function for Poisson−Boltzmann Solvation Methods. *J. Comput. Chem.* **2001**, *22*, 608−640.
(60) Lange, A. W.; Herbert, J. M.; Albrecht, B. J.; You, Z.-Q. Intrinsically Smooth Discretization of Connolly's Solvent-Excluded Molecular Surface. *Mol. Phys.* **2020**, *118*, No. e1644384.
(61) Jones, G.; Jackson, W. R.; Choi, C. Y.; Bergmark, W. R. Solvent Effects on Emission Yield and Lifetime for Coumarin Laser Dyes. Requirements for a Rotatory Decay Mechanism. *J. Phys. Chem.* **1985**, *89*, 294−300.
(62) Porel, M.; Klimczak, A.; Freitag, M.; Galoppini, E.; Ramamurthy, V. Photoinduced Electron Transfer Across a Molecular Wall: Coumarin Dyes as Donors and Methyl Viologen and TiO2 as Acceptors. *Langmuir* **2012**, *28*, 3355−3359.
(63) Ohio Supercomputer Center. http://osc.edu/ark:/19495/f5s1ph73.

https://dx.doi.org/10.1021/acs.jpcb.0c04032
J. Phys. Chem. B 2020, 124, 6998−7004